



## Fabrication of Polymeric Janus Particles by Droplet-Microfluidics

Journal:	<i>RSC Advances</i>
Manuscript ID:	RA-REV-01-2014-000158.R1
Article Type:	Review Article
Date Submitted by the Author:	18-Feb-2014
Complete List of Authors:	Lone, Saifullah; Kyungpook National University, Applied Chemistry, Engineering College

# Fabrication of Polymeric Janus Particles by Droplet Microfluidics

Saifullah Lone<sup>\*1,2</sup> and In Woo Cheong<sup>\*,2</sup>

<sup>1</sup> Division of Physical Sciences and Engineering, King Abdullah University of Science and Technology, Thuwal, 23955-6900, Saudi Arabia.

<sup>2</sup> Department of Applied Chemistry, Kyungpook National University, Daegu 702-701, South Korea.

**Abstract:** Janus particles (JPs), with their fascinating property of asymmetry, have received considerable attention in recent years in the fields of colloidal and particulate chemistry. The particles offer a range of exciting potential applications as they possess two distinctive parts with different chemistry, colors, polarities, and/or surfaces. Currently, a number of methodologies are available for the synthesis of JPs. This review presents a short description of polymeric JPs synthesized by droplet microfluidics.

## Saifullah Lone\*



*Dr. Saifullah Lone was born in India, and attained his Bachelor's and Master's degrees in Chemistry from India. He received his Ph.D. from Kyungpook National University, South Korea. Dr. Lone worked as a Post Doctoral Research Fellow at Seoul National University. He is currently working as a Post Doctoral Research Fellow at King Abdullah University of Science and Technology, Saudi Arabia. His research interests revolve around droplet microfluidics, Janus particles, encoding of smart polymeric microparticles & evaporative lithography.*

## In Woo Cheong\*



*Dr. In Woo Cheong received his Ph.D. degree in 2001 from Yonsei University, South Korea. He worked as a Post Doctoral Research Fellow in KCPC, University of Australia from 2002 to 2003. Afterwards, he worked as a research professor at Center for Nanotechnology, Yonsei University from 2003 to 2005, and then joined Kyungpook National University, South Korea, in 2005. He is currently an associate professor in the Department of Applied Chemistry, Kyungpook National University. His research interests include synthesis, self-assembly of stimuli-responsive copolymers, microfluidic particle preparation, and development of functional coatings, films, and adhesives.*

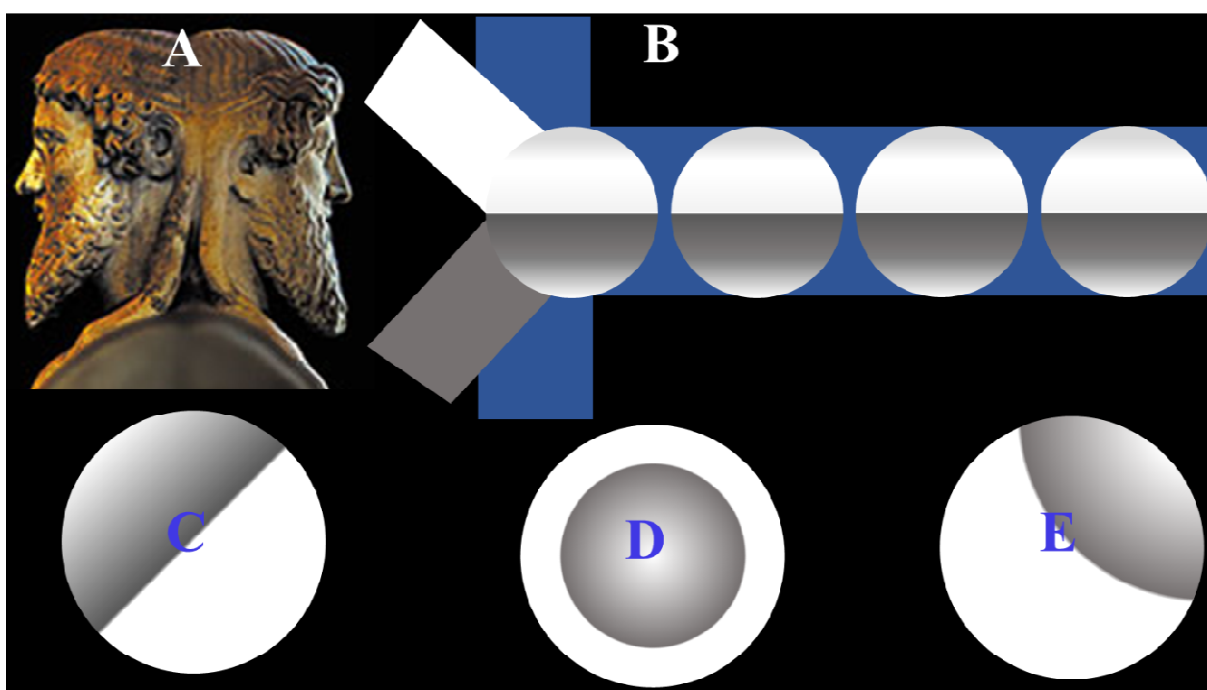
## 1. Introduction

Janus Particles (JPs) have been widely investigated over the past few decades because of their unique property of possessing two incompatible parts. The particles are named after the double-faced Roman god Janus. In Roman mythology, he is the god of gates, doors, beginnings, and endings; he is depicted with a double-faced head with each face looking in opposite directions. The concept originated in Asian culture (specifically in Daoism of the 6<sup>th</sup> century BC), symbolized by a black and white diagram of the Supreme Ultimate. In the field of scientific research, Lee and coworkers (Korea Advanced Institute of Science and Technology) reported the first Janus-like entities (poly(methyl methacrylate)/polystyrene composite particle latex materials) in 1985.<sup>1</sup>

The term “Janus particle” was coined by C. Casagrande in 1988 to describe spherical glass particles with hydrophilic and hydrophobic hemispheres.<sup>2</sup> The real popularity of JPs was heralded by P.G. Gennes in his prophetic 1991 Nobel lecture speech titled Soft Matter.<sup>3</sup> He coined the term “Janus grains,” and was one of the first scientists to use the word “Janus” to describe particles whose surfaces are different from a chemical point of view. Since then, the interest in JPs at both nano- and microscale has flourished, and the subject has attained popularity with researchers working in material and surface chemistry. A couple of review articles have been published on this topic.<sup>4,5</sup> However, a complete discussion on the significant contribution towards the preparation of JPs by droplet microfluidics is notably lacking. In this review, we focus specifically on the recent progress in the synthesis of asymmetric JPs by droplet microfluidics.

Janus entities have been prepared from dendrimers,<sup>6,7</sup> block copolymer micelles,<sup>8,9</sup> submicrometer-sized particles,<sup>10,11</sup> and micrometer-sized beads.<sup>12-24</sup> The potential applications of JPs are determined by the combination of the materials in the two different hemispheres. The application of JPs encompasses self-assembly, electronic paper, photonic materials, emulsion stabilization, imaging probes, sensors, building blocks for generating highly ordered lattices, three-dimensional electrical networks, flat-panel displays, rheological studies, medical treatments, and remote positioning in an electric field.<sup>25-36</sup> Thus, the need for

an effective method for producing JPs is now an urgent issue. Lately, various distinctive techniques, e.g., controlled coalescence of two distinct droplets followed by solidification of the merged phases, phase separation, toposelective surface modification, template-directed self-assembly, controlled surface nucleation, and hydrodynamic techniques have been employed for the preparation of JPs.<sup>37-53</sup> Among these techniques, droplet-based microfluidic methods have an outstanding edge over the rest as they offer a simple single-step, scalable strategy for preparation of JPs.



**Scheme 1** (A) Sculpture of Janus God, (B, C) schematic representation of co-flow microfluidic device and droplet formation, (C-E) schematic representation of Janus particles synthesized by co-flow mechanism, double emulsion and phase separation respectively.

Droplet microfluidics includes the preparation and manipulation of discrete micrometric entities (droplets, double emulsions, microcapsules, spheres, microbubbles, and JPs) inside microdevices at rates of up to twenty thousand per second. The approach allows for an independent control of each droplet/particle, thus generating microreactors that can be individually transported, mixed, and analyzed for biological and

chemical assays. Droplet microfluidics greatly reduces the volume of the required entities needed for the assays, thus enabling an easily affordable fabrication process for highly expensive materials used in chemical and biological analysis. This technology ensures that droplet fusion, fission, mixing, and sorting are done at a very high speed and precision. The method produces highly monodisperse droplets that are highly desirable in drug release kinetics. Microfluidic polymerization reactions conducted in droplets have also attracted enormous interest in the field of soft particulate materials. The technology has proven to be an excellent route to fabrication of polymer particles with unconventional shapes and morphologies (spheres, hemispheres, rods, disks, ellipsoids, and hollow or JPs). In this review, we provide an outline of the synthetic approaches used to fabricate JPs via droplet microfluidics. In this technique, there are usually three major flow regimes (co-flow, double emulsion, and phase separation) exploited to fabricate the JPs.

## 1. Janus particles by co-flow mechanism

**2.1. Bicolored JPs with electrical anisotropy.** The art of synthesizing JPs by the co-flow method originated in 2006, when Professor Toru Torii and co-workers at the University of Tokyo<sup>24</sup> reported the production of bicolored droplets containing two hemispheres—one black and the other transparent—using a flow-focusing-like geometry in a quartz glass microfluidic device. Two isobornyl acrylate streams, one doped with carbon black (black) and the other with titanium dioxide (white) in parallel laminar flow, were forced through a flow-focusing device to form droplets containing two distinct sections (Figure 1A). The symmetric recirculation of the organic fluids was induced at the end of the two-color fluid cylinder where the external aqueous streams co-flow (Figure 1B). These droplets were then polymerized via thermal polymerization into solid particles with distinctive hemispherical segments that exhibit two colors (Figure 1C). The particles were highly monodisperse and exhibited a coefficient of variation ( $CV$ ) less than 2%, as shown in Figure 1D. The authors also presented a brief account of the use of inorganic pigments for coloring to impart to the Janus spheres several advantages, e.g., better weather-resistant properties than can be achieved with organic dyes. In addition, carbon black and titanium oxide

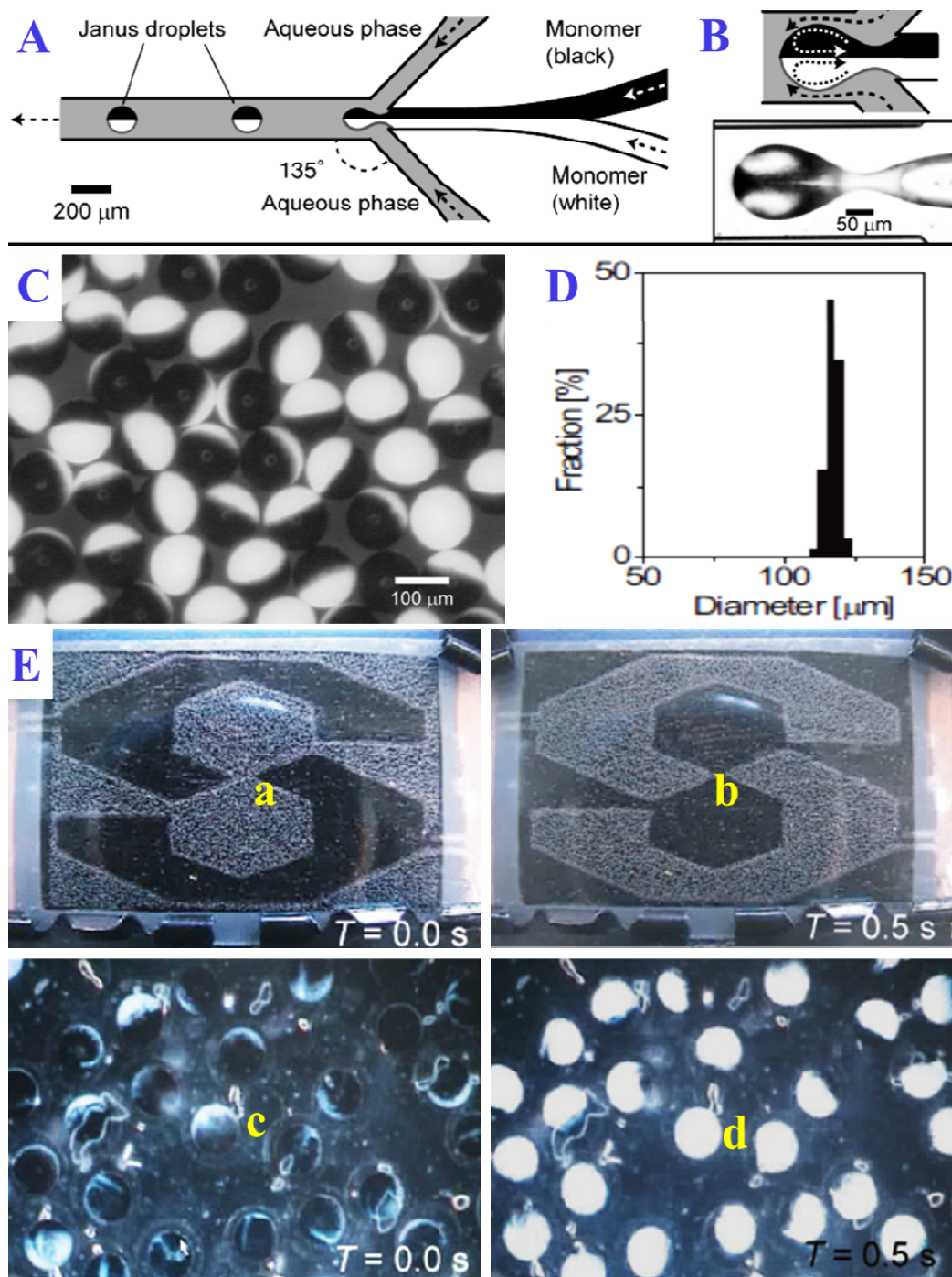


**Figure 1** (A) Schematic of the channel and flow configuration (B) Convection in the head of the organic fluid cylinder induced by the external aqueous stream. (C) Optical micrograph of monodisperse bicolor polymeric particles. (D) Size distribution of the particles. Mean diameter is 117 μm. CV is 1.9%. (E) Electrical actuation of the synthesized spheres: (a, b) Color switching test using prepared particles. A voltage of 100 V is applied between the 0.4 mm gap of two electrode panels (40 mm × 40 mm) at a switching frequency of 1 Hz. (c, d) Magnified top view of the display panel in (a, b). (Torri. et al. Copyright 2006 WILEY-VCH).

dispersed in two hemispheres have different charging properties, providing the surfaces of the engineered spheres with asymmetric charge distributions. To prove that the synthesized spheres are responsive to electric fields, the authors have reported on an electrical actuation of the JPs. A display panel was fabricated by a conventional method. In the presence of an external electric field, these spheres rotated such that their black hemispheres were oriented towards the negatively charged panel and vice versa. When the electric field gradient was reversed, the particles flipped (Figure 1E). To successfully fabricate Janus droplets composed of two miscible phases by the co-flow mechanism, it is necessary to consider both diffusive mixing and convective transport in microchannels. In this study, the Reynolds number ( $Re \ll 1$ ) is maintained at a low value so that no convective transport occurs across the two adjacent streams. Therefore, the method was projected to facilitate the future fabrication of a wide range of composites comprised of polymeric, ceramic, and metallic materials to create particles having various anisotropies designed through microfluidics. Particles with magnetic anisotropy might be readily created by dispersing magnetite ( $\text{Fe}_3\text{O}_4$ ) crystals in one hemisphere. Incorporation of a liquid-crystal phase could produce optically anisotropic particles.<sup>56,57</sup> “Barcoded” particles for biological multiplexing,<sup>58</sup> multicomponent carriers for targeted drug delivery,<sup>28</sup> and 3D photonic crystals of different domains<sup>59</sup> could also be promising applications.

**2.2. Janus and ternary particles.** In the previous discussion, there was no comprehensive control over the internal structure/surface composition of the microbeads. Additionally, the electrohydrodynamic and hydrodynamic focusing enhances mixing of the two phases, finally resulting in the preparation of particles with gradients that restrict the applications of JPs (e.g., their use as solar cell systems). Professor Kumacheva and co-workers from the University of Toronto, Canada, extended the idea of Professor Torii and co-workers by fabricating Janus and anisotropic ternary particles in a flow-focusing device.<sup>50</sup> Two liquid monomers (M1 and M2), each mixed with a photoinitiator, were made to flow in two central channels and focused by an aqueous solution of sodium dodecylsulfate (SDS), supplied via two side channels (Figure 2A). When a two-liquid thread is forced through an orifice, the thread breaks,

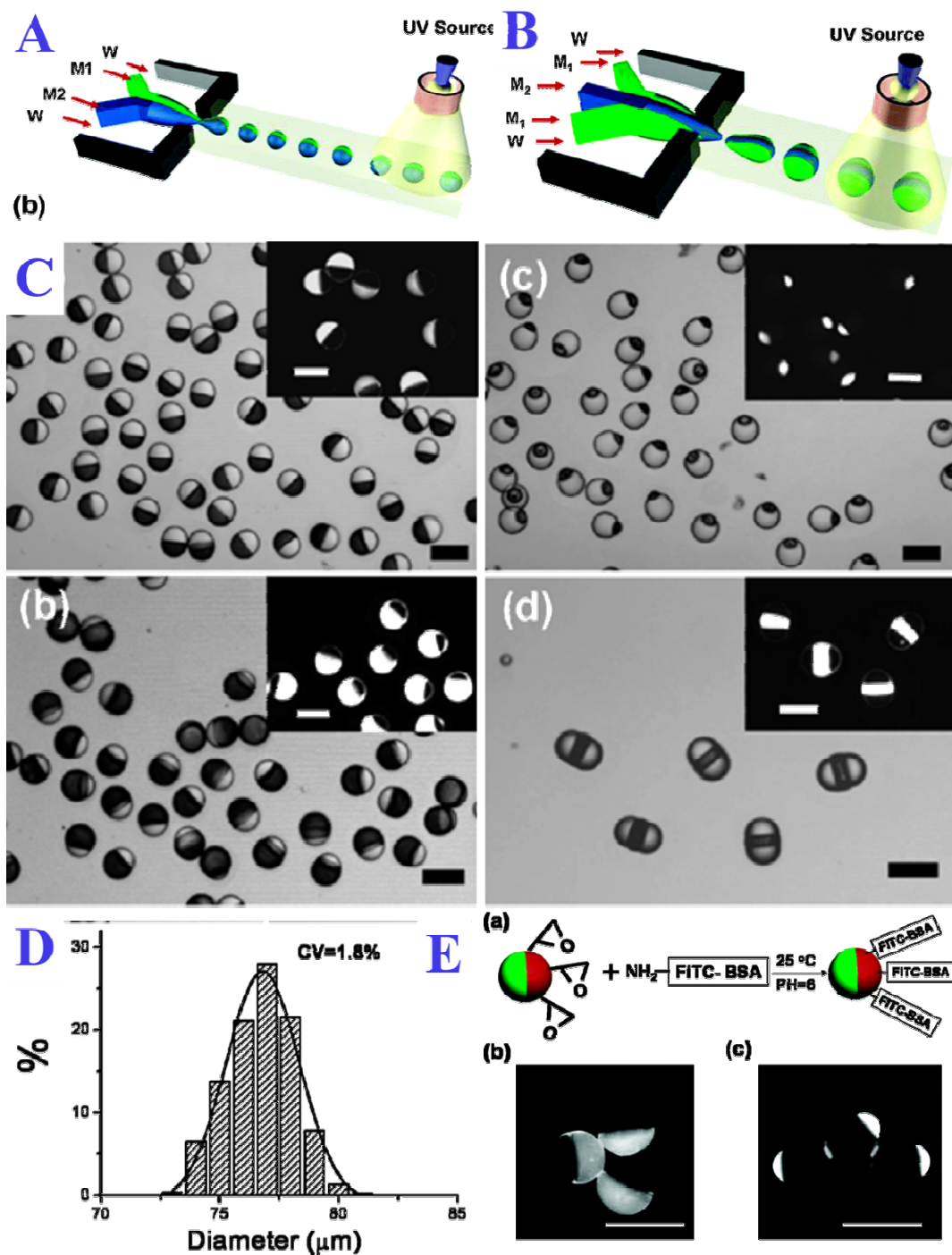
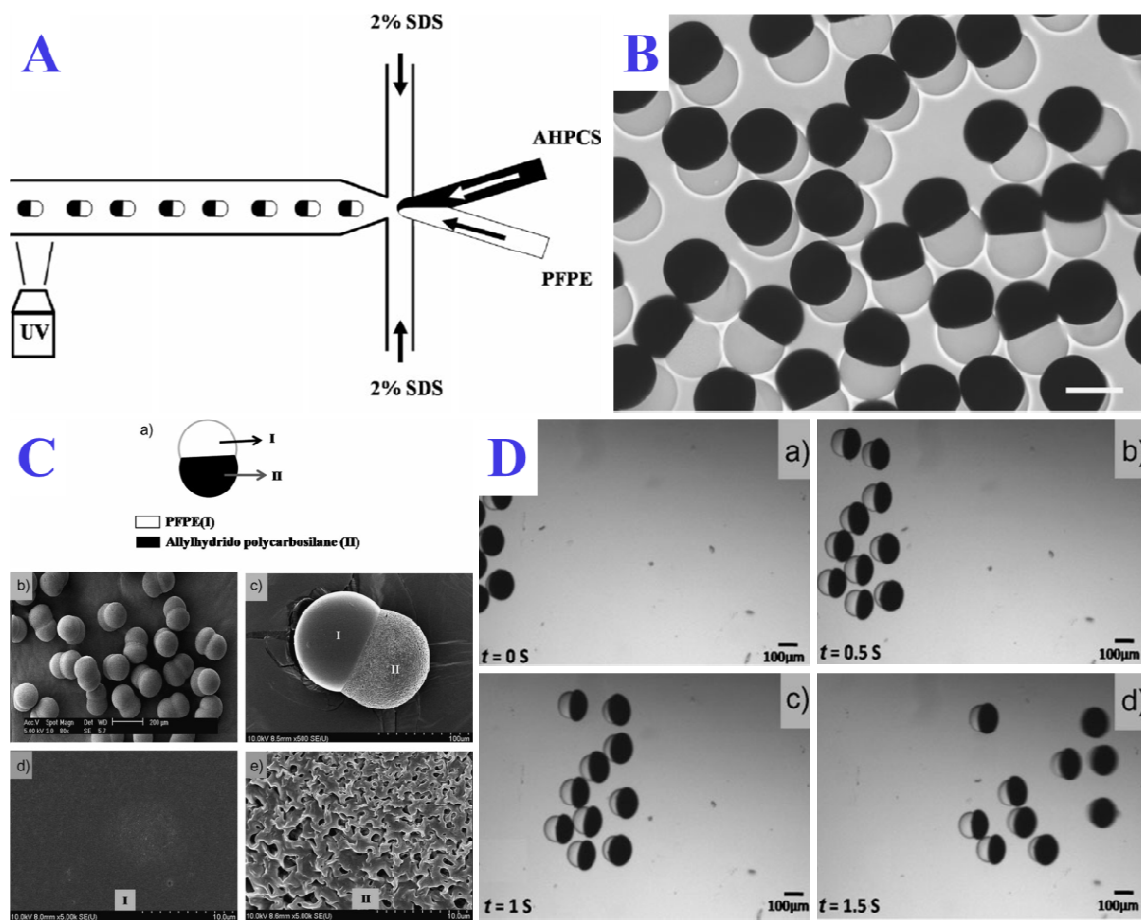


Figure 2 ((A)–(B)) Schematic illustration of the generation of Janus and ternary droplets. (C) Optical micrograph images of Janus and ternary particles with tunable anisotropy formed as shown in (A) and (B). (D) Size distribution of particles:  $CV = 1.8\%$ . (E) Selective functionalization of Janus particles (JPs) with FITC-BSA: (a) schematic of the reaction of bioconjugation. (b, c) JPs with different volume fractions of a hydrophilic phase asymmetrically bioconjugated with FITC-BSA. Bright phase: polymer obtained by polymerizing pentaerythritol triacrylate mixed with 16 wt% of glycidyl methacrylate. Scale bar: 100  $\mu\text{m}$ .  $\square_{\text{exc}} = 495 \text{ nm}$ , (Nie et al. Copyright 2006 American Chemical Society).

and droplets are formed and exposed to UV light in the downstream channel, thus initiating in situ free-radical polymerization of the monomer solution. By varying the flow rates of the aqueous and monomer solutions, different droplet sizes between 40 and 100  $\mu\text{m}$  are generated. The variations in the flow ratio of the two monomer solutions enable the creation of JPs with different fractions of monomers, as shown in Figure 2A. The technique can also be extended to the generation of ternary particles by introducing a third central channel. Alternatively, by supplying M1, M2, and M1 solutions into three channels respectively, ternary particles with respective alternating composition are obtained, as shown in Figure 2B. The polymers derived from M1 and M2 exhibit different hydrophobicities and different surface properties, which facilitate highly selective functionalization of the particles after microfluidic synthesis. The polymer JPs described by the authors carried different surface functionalities: a hydrophilic compartment of the microspheres contained carboxylic groups introduced by mixing M1 with acrylic acid. Moreover, the microfluidic synthesis of JPs reported in this work can well serve to produce carriers of different functionalities bound to the surfaces of the microbeads. The authors have demonstrated a highly selective functionalization of JPs by conjugating their hydrophilic compartment with the bovine serum albumin, as shown in Figure 2E. Epoxy groups are in the hydrophilic phase of JPs: microbeads carrying surface epoxy groups are ideal systems for protein immobilization via reactions with nucleophilic groups of proteins (e.g., amino, hydroxyl, or thiol moieties), accomplished with minimal chemical modification of the protein. The hydrophilic part of the JPs is prepared from pentaerythritol triacrylate mixed with 16 wt% of glycidyl methacrylate; the hydrophobic phase is synthesized from a methacryloxypropyl dimethylsiloxane. The Janus droplets were generated in the 2 wt% SDS aqueous solution at pH 6. The epoxy groups were stable on the time scale of the microfluidic experiment. Following polymerization of Janus droplets, the attached bovine serum albumin is covalently labeled with fluorescein isothiocyanate (FITC-BSA) to the surface of the JPs, as shown in Figure 2E (a). The reaction is carried out for 3 h at room temperature at pH 6. Figure 6E (b, c) presents the fluorescence microscopic images of asymmetrically bioconjugated JPs with localized different fractions of hydrophilic and hydrophobic localized regions. The method allows control over the surface area carrying bovine serum albumin by

changing the ratio of volume to surface area of each phase of the JPs.

**2.3. Inorganic–Organic Janus particles.** Researchers from Chungnam National University, South Korea, demonstrated a simple synthetic approach for the in situ preparation of monodisperse hybrid Janus microspheres (HJM) having organic and inorganic parts in a PDMS-based microfluidic device.<sup>51</sup> Based on the mechanism of shear-force-driven break-off, merged droplets of two photocurable oligomeric solutions with distinctive properties are generated in an immiscible continuous phase. Functionalized perfluoropolyether (PFPE) as the organic phase and hydrolytic allylhydridopolycarbosilane (AHPCS) as the inorganic phase are used for the generation of HJM in aqueous medium, with well-defined morphology and high monodispersity (average diameter of 162  $\mu\text{m}$  and a 3.5% coefficient of variation). The size and shape of the HJM is controlled by varying the flow rate of the dispersive and continuous phases. The HJM have two distinctive regions: a hydrophobic hemisphere (PFPE) having a smooth surface and a relatively hydrophilic region (AHPCS) with a rough, porous surface. In addition, pyrolysis and subsequent oxidation of these HJM convert them into SiC-based ceramic hemispheres through the removal of the organic portion and etching of the silica shell. It has been suggested that these porous, ceramic hemispheres may have potential as a catalytic bed for immobilizing metal ions used in high-temperature chemical processes. The selective incorporation of magnetic nanoparticles into the inorganic part illustrates the feasibility of the forced assembly of HJM in an applied magnetic field. Additionally, it is suggested that such magnetic JPs with appropriate modifications can be a very promising platform for various applications, such as in catalytic chemistry, biosensors, and biomedical processes.<sup>60-65</sup> Furthermore, the authors have designed a vertical dropping outlet to rapidly migrate the droplets downwards due to gravity; otherwise, the short residence time under UV irradiation in some of the microfluidic systems may lead to incomplete polymerization, which in turn may block the channels by collapsing the Janus droplets.



**Figure 3** (A) Schematic diagram of the microfluidic device used for the synthesis of hybrid Janus microspheres (HJM), (B) optical image of synthesized HJM with dumbbell shapes. (C) (a) Schematic illustration of the two lobes of a HJM. (b) SEM image of monodisperse HJM. (c) Enlarged image of a single HJM. Magnification of surfaces of the two different lobes of HJM. (d) The organic PFPE region (I) with a smooth surface. (e) The inorganic AHPCS (II) region with a rough, porous surface. (D) Optical images showing the frame-by-frame movement of magnetic HJM toward the magnetic field at different time sequences (direction of magnetic field is from left to right). (Prasad et al. Copyright 2009 WILEY-VCH).

**2.4. Multifunctional superparamagnetic Janus particles.** The art of generating monodisperse, spherical particles with anisotropic superparamagnetic responsiveness and homogeneous biphasic geometry shows promise for a range of potential applications ranging from fundamental studies on self-assembly to the development of photonic crystals and drug delivery systems. However, the synthesis of such particles has remained challenging. The utilization of methods, e.g., flame synthesis<sup>66</sup> and electrostatic<sup>67</sup> as well as

magnetostatic<sup>68</sup> nanoparticle phase separation in polymeric microparticles, have only succeeded in generating highly polydisperse particles characterized by ferromagnetic behavior and poorly defined Janus interfaces with particle-to-particle variation. Similarly, the synthesis of JPs using alginate chemistry is an alternative, but this is plagued by polydispersity,<sup>69</sup> an issue that complicates both the predictability and reproducibility of self-organized complex materials and their final effective properties. One way to overcome particle polydispersity involves evaporating a thin magnetic iron shell onto pre-existing polystyrene spheres.<sup>70</sup> The particles produced in this fashion are not bi-compartmental and also lack superparamagnetic behavior, a requisite property for predictable rapid-responsive field-driven assembly required for many biomedical applications such as detection in magnetic resonance imaging, separation, and drug delivery.<sup>71</sup> Thus, achieving efficient synthesis of monodisperse, bi-compartmental, and superparamagnetic JPs is of broad interest for many applications. Yuet et al., *Langmuir*, 2009,<sup>52</sup> reported the microfluidic synthesis of spherical Janus hydrogel particles with superparamagnetic properties and chemical anisotropy and their two-dimensional self-assembly into stable chain-like microstructures under an external magnetic field (Figure 4). They aimed to develop particles based on the following design criteria: (A) The particle comprises biocompatible, anti-biofouling polymer previously approved by the Food and Drug Administration (FDA) to facilitate future clinical implementation. (B) The particle assembles rapidly, anisotropically, and predictably in response to an external magnetic field. (C) The particle exhibits multifunctionality via compartmentalization of varying chemistries (e.g., DNA, fluorophores), enabling differential surface modification or environmental responsiveness. Although these biocompatible JPs find immediate use in tissue engineering, their ability to self-assemble with tunable anisotropic configurations make them an intriguing material for several exciting areas of research such as photonic crystals, novel microelectronic architecture, and sensing. With controllable compositions, these multifunctional microparticles offer a promising building block for engineering complex mesoscale assemblies with heterogeneous geometries and physicochemical properties.

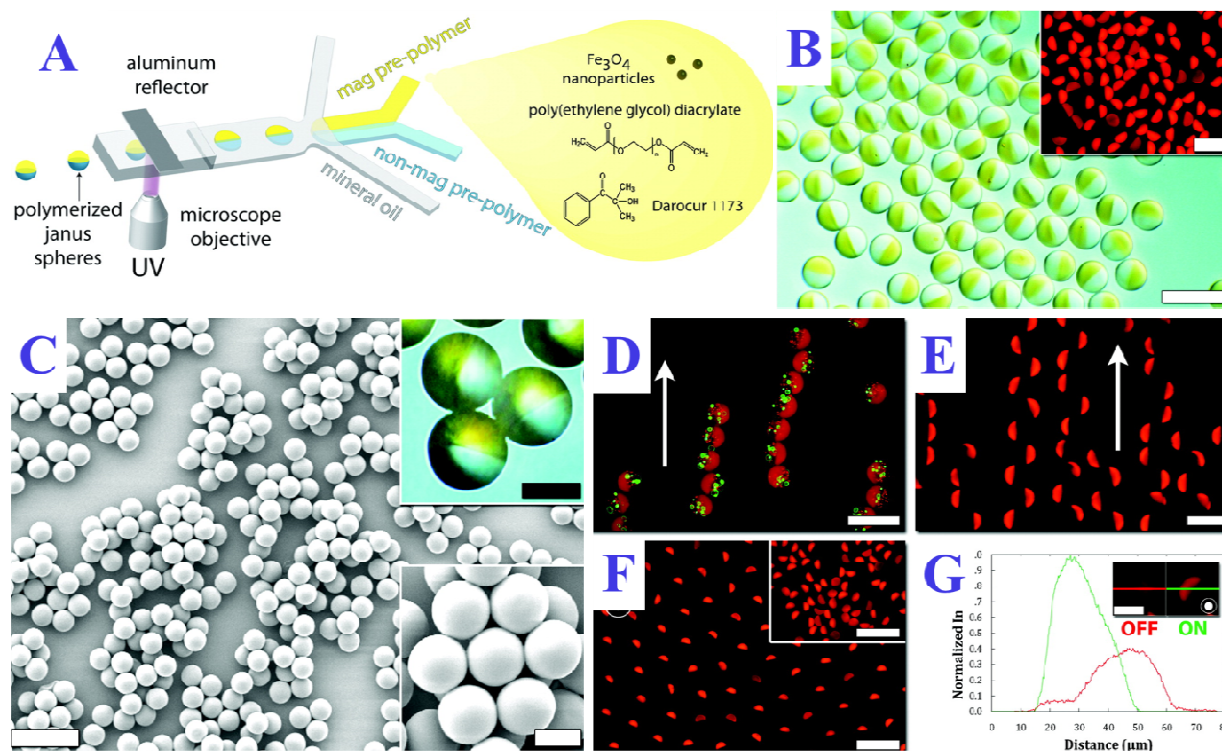


**Figure 4** (A) Schematic representation of Janus particle (JP) synthesis in a flow-focusing microfluidic device. (B) DIC and corresponding fluorescent (insert) images of magnetic JPs generated from co-flowing streams of polymer, one containing magnetic nanoparticles and the other containing Rhodamine B. The scale bars are 100  $\mu\text{m}$  wide. (C) SEM and DIC (upper right insert) images of dried JPs. The scale bars are 100  $\mu\text{m}$  wide and 25  $\mu\text{m}$  wide for the inserts. (D) Fluorescent image of self-assembling JPs containing 4.8  $\mu\text{m}$  wide yellow-green and 1  $\mu\text{m}$  wide red microspheres isolated in the nonmagnetic hemisphere. (E) Fluorescent image of self-assembling DNA-modified particles. The scale bars for panels A and B are 100  $\mu\text{m}$  wide. The applied fields in panels A and B are in-plane and  $14.7 \pm 0.1$  mT in magnitude. (F) Fluorescent images of JPs self-arranging from an initially disordered state (inset) following the application of an out-of-plane field ( $10.0 \pm 0.1$  mT). The scale bars for panel C are 200  $\mu\text{m}$  wide. (G) Normalized fluorescence intensity of a line scan of a selected JP before (OFF) and after (ON) field application (out-of-plane,  $10.0 \pm 0.1$  mT). The scale bar for the inset is 50  $\mu\text{m}$  wide (Yuet et al. Copyright 2010 American Chemical Society).

**2.5. Janus microgels from functional precursor polymers.** Over the years, the microfluidic technique has been extensively used to create Janus structures of various complexities. However, almost all of the previously published reports share an intrinsic limitation: since the microfluidic droplet template and the subsequent polymerization are coupled within a single step, flexibility in independently controlling the material properties and the morphology of the resultant microparticles is limited. Previously, microfluidic

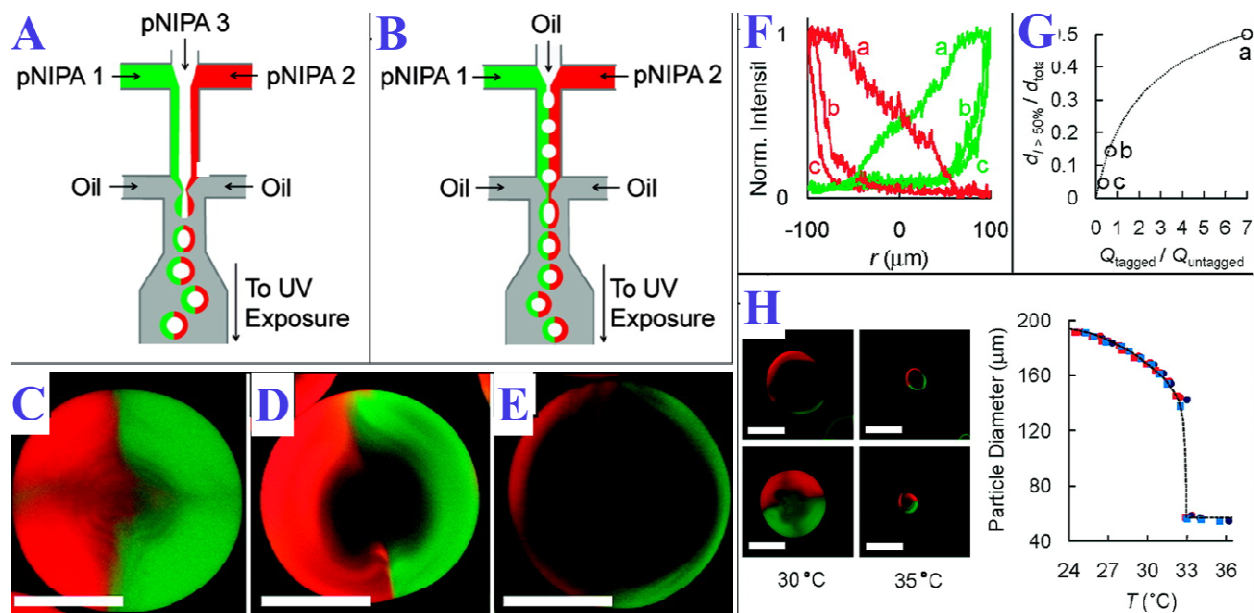


**Figure 5** (A) Schematic of a microfluidic device forming aqueous droplets from three independent semidilute PNIPAAm solutions. Right after droplet break up, the center phase (colorless PNIPAAm) is assembled in the core of the droplets, whereas the left- and right-flowing phases (green- and red-tagged PNIPAAm) form a Janus-shaped shell. (B) Characterization of PNIPAAm Janus microgels obtained from experiments as sketched in Figure 1(A). Varying the flow rates of the two tagged outer polymer phases, the untagged center polymer phase, and the emulsifying oil phase from (C) 105:105:30:500  $\mu\text{L h}^{-1}$  over (D) 50:50:150:500  $\mu\text{L h}^{-1}$  to (E) 30:30:180:500  $\mu\text{L h}^{-1}$  yields particles with different inner morphology. (F) Spatially resolved profiles of the normalized fluorescence intensity across the resultant particles (presented as moving averages of five sequential data points, respectively). (G) Relative diameter of the tagged shell of the microgels,  $d_{l > 50\%}/d_{\text{total}}$ , as a function of the ratio of flow rates of the tagged and untagged polymer phases,  $Q_{\text{tagged}}/Q_{\text{untagged}}$ . Circles represent experimental data as derived from the intensity profiles in panel (d), while the dotted line is calculated theoretically as detailed in the main text. (H) Thermo-responsive behavior of the Janus microgels shown in Panel (A) and (C). The micrographs on the left side show two particles with a high (upper row) and low (lower row) content of tagged precursor polymers in a swollen (left column) and shrunken (right column) state. The right-hand diagram details the particle diameter as a function of temperature. Circles represent the Janus particles shown in the lower row, whereas squares refer to the particles shown in the upper row. Red and blue symbols represent successive heating and cooling cycles. The dotted line is drawn manually to guide the eye. All scale bars denote 100  $\mu\text{m}$  (Seiffert et al. Copyright 2010 American Chemical Society).

approaches created JPs with rough modifications on both parts, either by nesting different mesoscopic additives into one common, rapidly curing polymer matrix<sup>26,27,54</sup> or by using fundamentally different materials for forming both parts.<sup>52</sup> Recently, Seiffert et al., *Langmuir*, 2010,<sup>70</sup> proposed with an impressive idea to overcome this limitation, thus maximizing the use of JPs prepared by microfluidics.

They prepared Janus shaped microgel particles from cross-linkable precursor polymers by using droplet microfluidics. To demonstrate the anisotropic incorporation of these precursors into the resultant microgels, they tagged them with fluorescent dyes, representing arbitrary functional sites. These dyes are easy to detect and allowed them to visualize the spatial distribution of the modified precursor polymers inside the microgel particles. They also took advantage of the control offered by the microfluidic droplet template to fabricate hollow microcapsules with two different parts (Janus shells), and extended their approach by complexing Janus microgels made from macromolecular precursors with a ferromagnetic additive, thus allowing for remote actuation of the microgels (Figure 5). The polymer-analogous microgel formulation technique presented in this article is thus a versatile way of producing micrometer sized hydrogel particles with an asymmetric modification. Since the precursor polymers used to form them can be functionalized prior to the microgel formation, highly controlled microfluidic templating can be combined with the great flexibility of preparative polymer chemistry, allowing bifunctional or anisotropic microgels to be produced with precisely determined properties. The art of loading these particles with functional additives, such as ferromagnetic nanoparticles, combines the asymmetric modification of the polymer shell with the functionality of the additive. The authors go on to claim that the microfluidic devices used in this work are made by soft lithography, the method can be conducted on a larger scale, offering the potential to produce larger quantities of new anisotropic microparticles.

### **3. Janus particles from double emulsion**

**3.1 Janus particles templated from double emulsion droplets.** All of the previously reported examples of microfluidically fabricated JPs are composed of two hydrogel phases and are made from two dissimilar but completely miscible hydrophilic monomer streams. Although the techniques can be extended to fabricate JPs from immiscible fluids, the values of the interfacial tension between the fluids need to be within a certain range. Outside of that range, the two “halves” of the JPs do not stick to each other to produce individual droplets. Thus, fabrication of JPs from a broad range of immiscible fluids requires new microfluidic techniques. This should expand the portfolio of chemicals that can be used for shaping

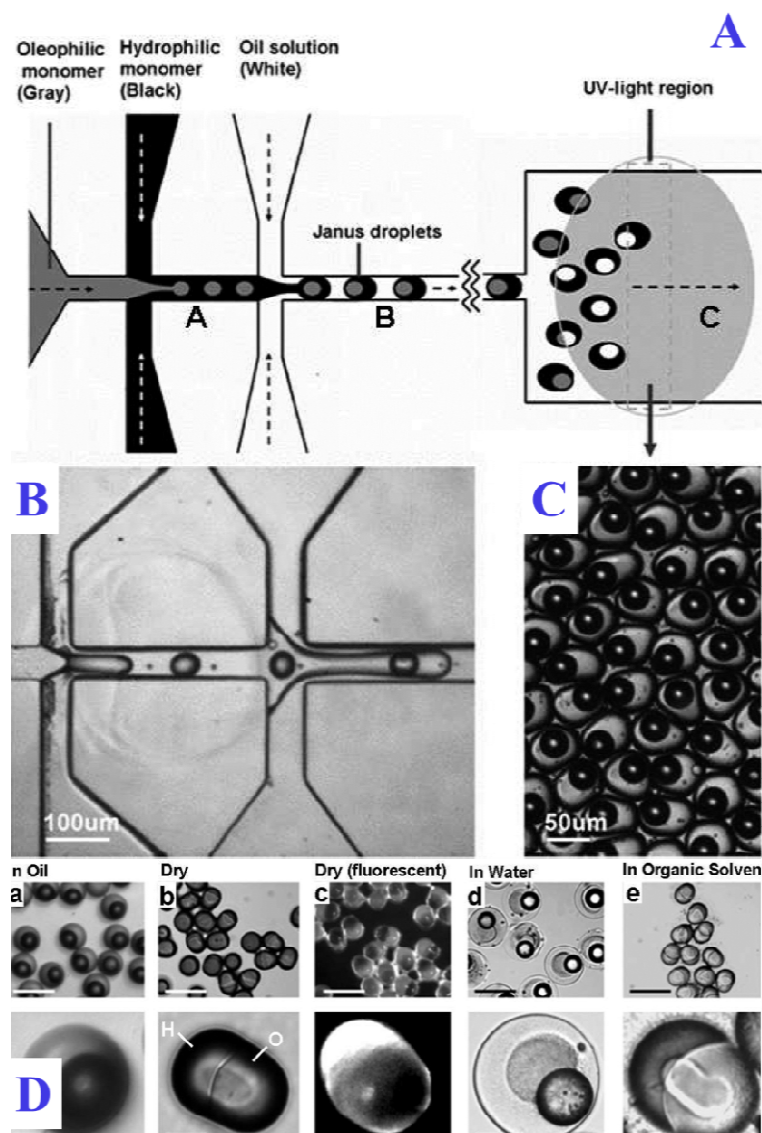


**Figure 6.** (A) Schematic representation of PDMS double emulsion device. (B) Photomicrograph of the PDMS device for fabricating double-emulsion droplets. The double-emulsion droplets consist of an organophilic monomer core (gray) that is encapsulated by a water monomer droplet (black) in fluorocarbon oil (white). The thickness of the channel is 50  $\mu\text{m}$ . (C) A collection of these double emulsions in a large channel on the same device, where they are exposed to a UV beam, which initiates polymerization of the monomers and locks in the anisotropic Janus structure and (C) SEM image of an organophilic-hydrophilic Janus particle (JP). The two halves of the JP are spherical due to the spherical shape of the double-emulsion drops from which it is templated. The size of the two halves can be adjusted by controlling the flow rates of the fluids forming the double emulsions. (D) Photomicrograph of the organophilic-hydrophilic JPs (a) dispersed in fluorocarbon oil, (b,c) dried, (d) dispersed in water, and (e) dispersed in acetone. The images below show magnified views of individual JPs (left, identified as H, hydrophilic lobe; right, identified as O, organophilic lobe). The scaling bar in the top row is 100  $\mu\text{m}$ , and the scaling bar in the bottom row is 20  $\mu\text{m}$ , (Chen et al. Copyright 2009 American Chemical Society).

the two parts of the JPs and result in the fabrication of particles with more diverse properties, thus finally leading to several new applications. Professor David A. Weitz and co-workers are at the forefront of fabricating exciting microfluidic microparticles with different morphologies and a wide range of applications. They were the first to generate JPs from double emulsion templates.<sup>71</sup> This work was carried out in a PDMS double emulsion device (Figure 6). The microfluidic device employed in this work was made from a silicon elastomer of PDMS using soft-lithography methods. The channels were coated with a sol gel layer functionalized with photoreactive silanes. This chemical treatment allows the wettability of the channels to be spatially patterned and thus allows the formation of double-emulsion droplets<sup>72</sup> as reported by the authors. One critical point is that while generating double emulsified droplets inside a microfluidic device, the inner droplets are not fixed at the middle of the droplets due to fluid flow induced by viscous forces within the double emulsified droplets and the difference between the densities of the two fluids. If the diameter of the double emulsified droplets is larger than the height of the channel, the droplets will be deformed into non-spherical shapes while flowing through the channels. Non-spherical particles can be formed by locking in the structure of the double emulsified droplets and is therefore achieved easily by solidification of the droplets through photo-polymerization.<sup>73</sup> The authors have successfully demonstrated this facile technique of fabricating JPs with a hydrophilic and an organophilic part. Such particles possess tremendous potential for the simultaneous transportation and release of both hydrophilic and organophilic macromolecules. This approach combines the high degree of control offered by droplet microfluidics with the ability to tune the particle chemistry to fabricate non-spherical particles. It is also very simple and is independent of the choice of monomer, as long as an appropriate polymerization strategy is available. Therefore, this approach offers the possibility to choose the materials of the non-spherical particles according to the requirements of the specific application.

**3.2. Magnetic hydrogel particles with uniform anisotropic structure.** By utilizing the double emulsion approach, Professor David A. Weitz and co-workers furthermore produced magnetic hydrogel particles with uniform anisotropic internal structure by a flow-focusing drop maker using double emulsions as

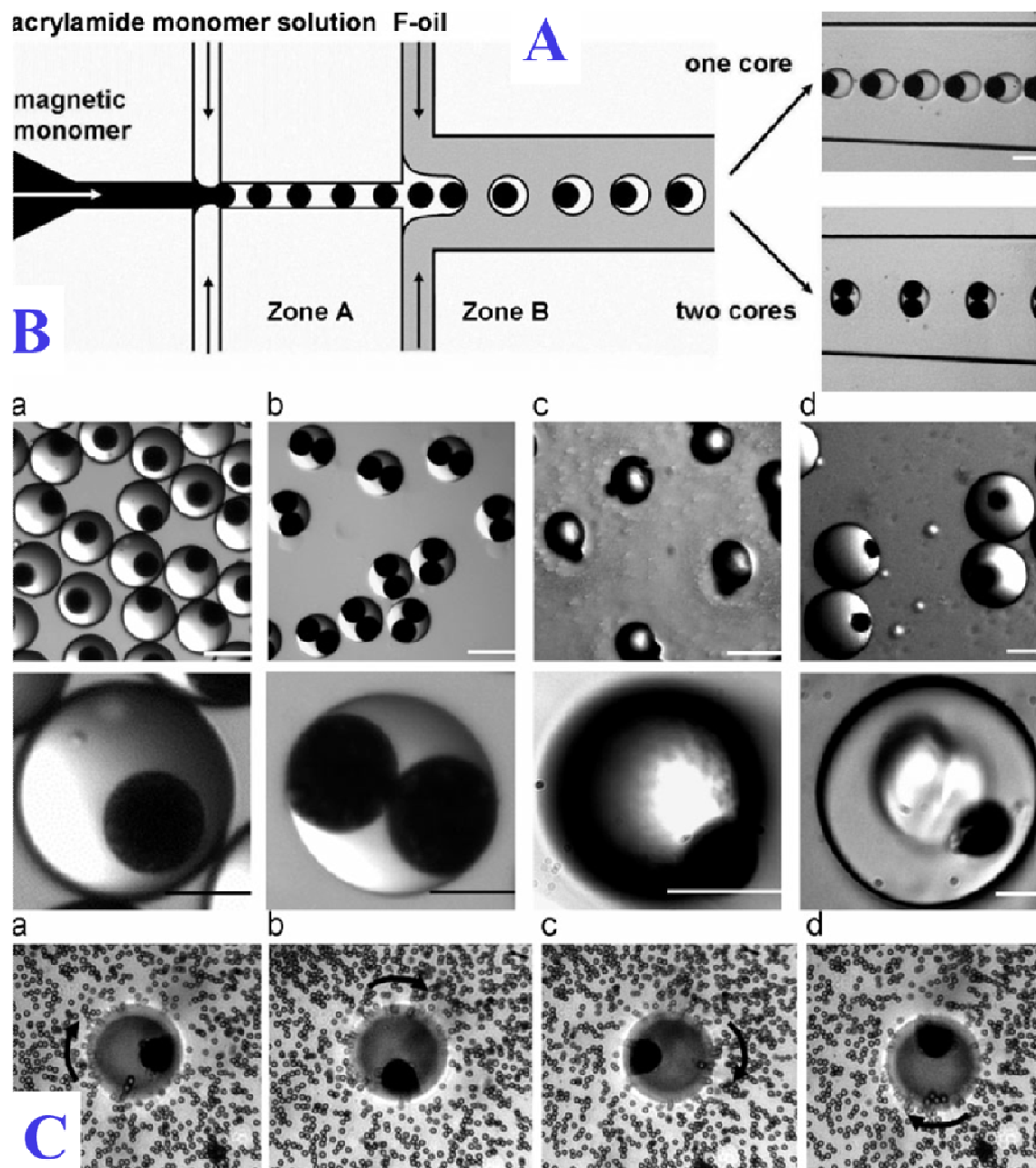


**Figure 7** (A) Scheme of the PDMS device for forming double emulsion droplets. The droplets consist of the hydrophobic monomer core with magnetic material (black) that is encapsulated by a hydrophilic monomer droplet (white) suspended in fluorocarbon oil (gray). By increasing the inner flow rate, two magnetic cores can be encapsulated in the droplets. The scale bar for the two images corresponds to 50  $\mu\text{m}$ . (B) Optical microscopy images of magnetic gel particles with uniform anisotropic features: a) Particles with a single magnetic core, and b) with two magnetic cores, in fluorocarbon oil. c) Single-core particles dried, and d) re-dispersed in water. The images in the second row show magnified views of the same particles. The scale bar in the top row is 50  $\mu\text{m}$  and in the bottom row is 20  $\mu\text{m}$ . (C) A series of optical microscopy images, showing the particle rotating around its magnetic bead (Chen et al. Copyright 2009 WILEY-VCH).

templates,<sup>74</sup> Figure 7. Moreover, with the advantage of a double emulsion core-shell structure, the inorganic magnetic inserts were fully covered by a biocompatible polymer network, which allows the particles to be used in biomedical applications. Microfluidic assembly by using flow-focusing double emulsion drop makers provides excellent control over the size, morphology, and monodispersity. The particles exhibit excellent rotational control by an external field, with the possibility of eccentric rotation inducing a significant localized shear flow. The authors suggested that the unique magnetic response of magnetic hydrogel particles with internal anisotropy has great potential for many microfluidic applications. In particular, the asymmetric particles offer a possibility for eccentric rotation and thus inducement of significant shear flow in the vicinity of each particle, with the potential for micro-mixing of fluids, e.g., in a microfluidic reactor or directly in vivo. Additionally, the authors have claimed that these particles could serve as probes for micro-rheological characterization of complex fluids and biomaterials. Finally, biocompatibility and the capacity to modify the anisotropic internal microstructure within the generic core-shell morphology offer new opportunities in biomedical applications.

#### **4. Janus particles by phase separation**

**4.1. 1. Janus particles by phase separation of nanoparticles.** The principles for fabricating the majority of the polymer JPs via droplet microfluidics are similar to those for fabricating homogeneous particles; however, instead of a flowing single stream of monomer, two separate streams are co-flowed through the same device channel. The successful microfluidic fabrication of JPs is assured by the parallel flow of monomer streams at all times before the particle morphology is locked, any disturbances can lead to cross-mixing of the fluids and to the formation of particles with a mixed internal morphology instead of particles with two distinct parts.<sup>31</sup> Moreover, the interface between the two fluids must be stable and independent of both time and space; this requires both fluids to be miscible and therefore, limits the range of chemicals that can be employed. To address this problem, Professor Weitz's group presented a microfluidic approach to fabricate JPs with a novel, highly anisotropic, and finely tunable internal architecture<sup>65</sup> (Figure 8). The resulting particles consisted of one part composed of a hydrogel and the

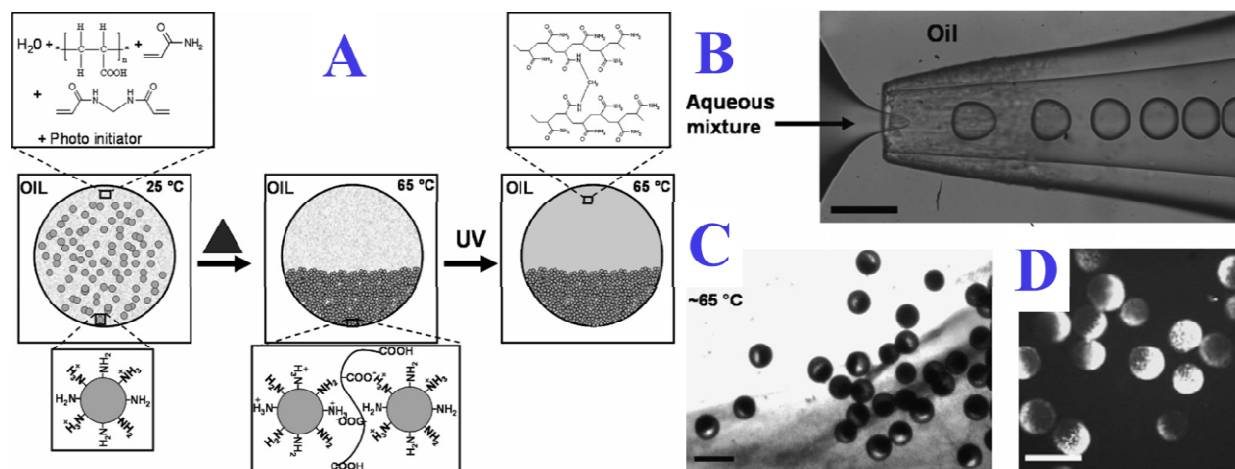


**Figure 8.** (A) Schematic representation of the process employed for making Janus particles. Aqueous droplets containing the cationic PNIPAAm microgels, polyacrylic acid, acrylamide, methylene bisacrylamide, and a photoinitiator are formed in silicon oil. Upon heating, the microgels shrink and aggregate on one side of the droplet under the combined influence of the high temperature and the electrostatic interactions between them and the polyacrylic acid. The acrylamide monomer forced into the other side of the droplets is then polymerized and gelled using ultraviolet light to form Janus gel particles whose one part is composed of acrylamide and the other part is composed of PNIPAAm microgels. (B) Formation of monodisperse droplets in a microfluidic device with a flow-focusing geometry. The dispersed phase is an aqueous suspension composed of cationic PNIPAAm microgels, polyacrylic acid, and photopolymerizable monomers while the continuous phase is constituted of silicon oil containing a surfactant. (C) Aggregation and compaction of the PNIPAAm microgels on one side of the droplets upon heating the emulsion at 65 °C. (D) A fluorescent microscope image of Janus particles formed by photopolymerizing the monomers in the phase-separated droplets. The scale bars are 200 nm (Shah et al. Copyright 2009 WILEY-VCH).

other part composed predominantly of aggregated colloidal nanoparticles. The creation of JPs with such a unique internal morphology is facilitated by the induced phase separation of colloidal nanoparticles in droplets. The synthesis of JPs by heat induced phase separation of nanoparticles in droplets by flowing one stream of monomer solution in continuous phase is shown in Figure 8. First, droplets are prepared using a microfluidic device; the droplets are then heated for phase separation and finally the phase-separated anisotropic droplets are fixed by UV-irradiation. The authors also reported magnetized JPs by the incorporation of magnetic nanoparticles into one half to enhance the functional dichotomy of the particles and to tailor them to suit specific applications.

**4.2. Janus particles by UV-directed phase separation.** To make significant progress in quantity and monodispersity, our group has recently further extended and simplified the approach by offering an easy single step microfluidic approach to synthesize polymer JPs.<sup>53</sup> The idea is built from our previous study,<sup>75</sup> where we explained the UV-Vis directed reversible phase separation of light sensitive polymer in the absence of polymerization. The JPs are templated from homogenous photopolymerizable water-in-oil (W/O) emulsion. This emulsion, when subjected to UV irradiation, undergoes phase separation of light sensitive random copolymers to create the JPs. The aqueous mixture consisting of light responsive random copolymer (PNIPAAm-co-SPO-co-fluorophore) along with *N,N'*-methylenebisacrylamide (MBA) as a cross-linking agent is constricted to fabricate monodisperse aqueous droplets in continuous phase of hexadecane, Span 80, and 2,2-diethoxyacetophenone (DEAP). In this study, the asymmetric particles are prepared by two processes: UV-induced phase separation of light-sensitive polymer in W/O emulsion and polymerization of MBA at the interface. The driving force for polymer aggregation originates from the photo-induced heterolytic cleavage of the C (spiro)-O bond of SPO under UV light. The cleavage reaction leads to an open (merocyanine) structure of zwitterions (Figure 9(Ba)), which eventually gives rise to inter- and intra-chain ionic and hydrogen bonding interactions in the presence of MBA or DEAP. Therefore, the polymer shrinks to expel water molecules. The strong forces of attraction within the polymer chains create asymmetry in the W/O droplet (Figure 9(Bb)). Meanwhile, the DEAP dissolved in the hexadecane generates a large number of initiator radicals. These active free-radicals then diffuse across the hexadecane–aqueous droplet of poly(NIPAAm-co-SPO-co-fluorophore) and the MBA monomer interface. As the light sensitive polymer is already phase separated by the zwitterionic pair effect, the remaining MBA dissolved in the aqueous phase also diffuses towards the water–hexadecane interface and induces polymerization. Consequently, a thin cross-linked poly(MBA) layer forms at the interface and can be clearly seen as a thin lining around the main body of the JPs. It is predicted that the method is facile and can be scaled up for massive production of JPs.



elegantly delivers the easiest way to impart specific physical characteristics in the anisotropic particles and synthesize a range of anisotropic particles with a broad spectrum of potential applications. Despite all these benefits, the droplet-based microfluidic (co-flow, double emulsion template, and phase-separation-induced) approach to fabricate polymer JPs has a serious problem regarding the preparation of a limited number/class of anisotropic particles at the microscale. As nanoscale applications are now of greater interest, researchers studying droplet microfluidics are facing an immediate need for fabrication of nanosized symmetric/asymmetric polymer particles. Thus, though the field has shown enormous promise in such a short period, reducing the size of the fabricated particles to the nanoscale is imperative; otherwise, the approach of droplet microfluidics to fabricate symmetric/asymmetric polymer particles will have a limited scope of applications.

### Acknowledgements

This work was supported by the Ministry of Trade, Industry and Energy (No. 10044338), Pioneer Research Center Program of the National Research Foundation of Korea funded by the Ministry of Education, Science and Technology (2010-0019308) and Coway through Cosmetics Research Center (2013). Additional, authors are highly thankful to Prof. Sughoon Kwon at Seoul National University for funding & valuable discussions.

### Notes and References

1. I. Cho and K. W. Lee. *J. Appl. Polym. Sci.*, 1985, **30**, 1903–1926.
2. C. Casagrande, P. Fabre, E. Raphael and M. Veyssié. *Europhys. Lett.*, 1989, **9**, 251–255.
3. P. G. D. Gennes, *College of France*, 1991.
4. A. Walther and A. H. E. Müller, *Soft Matter*, 2008, **4**, 663–668.
5. F. W. and A. F. M. Kilbinger\* *Angew. Chem. Int. Ed.*, 2009, **48**, 8412–8421.
6. J. Ropponen, S. Nummelin, K. Rissanen, *Org. Lett.*, 2004, **6**, 2495–2497.
7. V. Percec, M. R. Imam, T. K. Bera, V. S. K. Balagurusamy, M. Peterca, P. A. Heiney, *Angew. Chem., Int. Ed.*, 2005, **44**, 4739–4745.
8. J. Wang, G. Liu, G. Rivas, *Anal. Chem.*, 2003, **75**, 4667–4671.
9. R. Erhardt, M. F. Zhang, A. Böcker, H. Zettl, C. Abetz, P. Frederik, G. Krausch, V. Abetz, A. H. E. Müller, *J. Am. Chem. Soc.*, 2003, **125**, 3260–3267.
10. Y. Z. Du, T. Tomohiro, G. Zhang, K. Nakamura, M. Kodaka, *Chem. Commun.*, 2004, **5**, 616–617.

11. K. H. Roh, D. C. Martin, J. Lahann, *Nat. Mater.*, 2005, **4**, 759–763.
12. O. Cayre, V. N. Paunov, O. D. Velev, *J. Mater. Chem.*, 2003, **13**, 2445–2450.
13. O. Cayre, V. N. Paunov, O. D. Velev, *Chem. Commun.*, 2003, **18**, 2296–2297.
14. V. N. Paunov, O. Cayre, *J. Adv. Mater.*, 2004, **16**, 788–791.
15. J. C. Love, B. D. Gates, D. B. Wolfe, K. E. Paul, G. M. Whitesides, *Nano Lett.*, 2002, **2**, 891–894.
16. M. A. Correa-Duarte, V. Salgueirino-Maceira, B. Rodriguez-Gonzalez, L. M. Lizmarzan, A. Kosiorek, W. Kandulski, M. Giersig, *Adv. Mater.*, 2005, **17**, 2014–2018.
17. H. Takei, N. Shimizu, *Langmuir*, 1997, **13**, 1865–1868.
18. E. Hugonnot, A. Carles, M. H. Delville, P. Panizza, J. P. Delville, *Langmuir*, 2003, **19**, 226–229.
19. Y. Nonomura, S. Komura, K. Tsujii, *Langmuir*, 2004, **20**, 11821–11823.
20. O. D. Velev, A. M. Lenhoff, E. W. Kaler, *Science* 2000, **287**, 2240–2243.
21. T. Nisisako, T. Torii, T. Higuchi, *J. Chem. Eng.*, 2004, **101**, 23–29.
22. K. Fujimoto, K. Nakahama, M. Shidara, H. Kawaguchi, *Langmuir* 1999, **15**, 4630–4635.
23. A. Perro, S. Reculosa, S. Ravaine, E. Bourgeat-Lami, E. Duguet, *J. Mater. Chem.*, 2005, **15**, 3745–3760.
24. T. Nisisako, T. Torii, T. Takahashi, Y. Takizawa, *Adv. Mater.*, 2006, **18**, 1152–1156.
25. S.-H. Kim, S.-J. Jeon, W. C. Jeong, H. S. Park, S.-M. Yang, *Adv. Mater.*, 2008, **20**, 4129–4134.
26. K. H. Roh, D. C. Martin, J. Lahann, *Nat. Mater.*, 2005, **4**, 759–763.
27. Y. Lu, Y. Yin, Y. Xia, *Adv. Mater.* 2001, **13**, 415.
28. D. H. Gracias, J. Tien, T. L. Breen, C. Hsu, G. M. Whitesides, *Science*, 2000, **289**, 1170.
29. T. Nisisako, T. Torii, T. Takahashi, Y. Takizawa, *Adv. Mater.*, 2006, **18**, 1152.
30. A. Donev, I. Cisse, D. Sachs, E. A. Variano, F. H. Stillinger, R. Connelly, S. Torquato, P. M. Chaikin, *Science*, 2004, **303**, 990.
31. C. F. Brooks, G. G. Fuller, C. W. Frank, C. R. Robertson, *Langmuir*, 1999, **15**, 2450.
32. <http://www.physorg.com/news6811.html>.
33. O. Cayre, V. N. Paunov, O. D. Velev, *J. Mater. Chem.*, 2003, **13**, 2445–2450.
34. O. Cayre, V. N. Paunov, O. D. Velev, *Chem. Commun.*, 2003, **18**, 2296–2297.
35. V. N. Paunov, O. Cayre, *J. Adv. Mater.* 2004, **16**, 788–791.
36. J. R. Millman, K. H. Bhatt, B. G. Prevo, O. D. Velev, *Nat. Mater.*, 2005, **4**, 98–102.
37. M. Fialkowski, A. Bitner, B. A. Grzybowski, *Nat. Mater.*, 2005, **4**, 93–97.
38. H. Gu, R. Zheng, X. Zhang, B. Xu, *J. Am. Chem. Soc.*, 2004, **126**, 5664–5665.
39. U. Akiva, S. Margel, *Colloids Surf. A*, 2005, **253**, 9–13.
40. J. C. Love, B. D. Gates, D. B. Wolfe,; K. E. Paul, Whitesides, G. M. *Nano Lett.*, 2002, **2**, 891–894.
41. M. A. Correa-Duarte, V. Salgueirino-Maceira, B. Rodriguez-Gonzalez, L. M. Lizmarzan, A. Kosiorek, W. Kandulski, M. Giersig, *Adv. Mater.*, 2005, **17**, 2014–2018.
42. H. Takei, N. Shimizu, *Langmuir*, 1997, **13**, 1865–1868.
43. E. Hugonnot, A. Carles, M. H. Delville, P. Panizza, J. P. Delville, *Langmuir*, 2003, **19**, 226–229.
44. K. Fujimoto, K. Nakahama, M. Shidara, H. Kawaguchi, *Langmuir*, 1999, **15**, 4630–4635.
45. Y. Yin, Y. Lu, Y. Xia, *J. Am. Chem. Soc.*, 2001, **123**, 771–772.
46. Y. Yin, Y. Lu, B. Gates, Y. Xia, *J. Am. Chem. Soc.*, 2001, **123**, 8718–8729.
47. Y. Xia, Y. Yin, Y. Lu, J. McLellan, *Adv. Funct. Mater.*, 2003, **13**, 907–918.
48. H. Yu, M. Chen, P. M. Rice, S. X. Wang, R. L. White, S. Sun, *Nano. Lett.*, 2005, **5**, 379–382.
49. S. Reculosa, C. Poncet-Legrand, S. Ravaine, C. Mingotaud, E. Duguet, E. Bourgeat-Lami, *Chem. Mater.*, 2002, **14**, 2354–2359.

50. Z. Nie, W. Li, M. Seo, S. Xu, and E. Kumacheva, *J. Am. Chem. Soc.*, 2006, **128**, 9408–9412.
51. N. Prasad, J. Perumal, C. H. Choi, C. S. Lee and D. P. Kim, *Adv. Funct. Mater.* 2009, **19**, 1656–1662.
52. K. P. Yuet, D. K. Hwang, R. Haghgooye, and P. S. Doyle, *Langmuir*, 2010, **26**, 4281–4287.
53. S. Lone, S. H. Kim, S. W. Nam, S. Park, J. Joo and I. W. Cheong, *Chem. Commun.*, 2011, **47**, 2634–2636.
54. A. Fernández-Nieves, G. Cristobal, V. Garcés-Chávez, G. C. Spalding, K. Dholakia, D. A. Weitz, *Adv. Mater.*, 2005, **17**, 680.
55. A. Fernández-Nieves, *Soft Matter*, 2006, **2**, 105–108.
56. N. H. Finkel, X. Lou, C. Wang, L. He, *Anal. Chem.*, 2004, **76**, 352A.
57. J. R. Millman, K. H. Bhatt, B. G. Prevo, O. D. Velev, *Nat. Mater.*, 2005, **4**, 98.
58. R. K. Paul, K.-H. Lee, H.-D. Kim, B.-T. Lee, *J. Am. Ceram. Soc.*, 2008, **91**, 2509.
59. L. Lianos, A. Berthet, C. Deranlot, F. J. Cadete Santos Aires, J. Massardier, J. C. Bertolini, *J. Catal.* 1998, **177**, 129.
60. T. A. Taton, C. A. Mirkin, R. L. Letsinger, *Science* 2000, **289**, 1757.
61. A. Jordan, R. Scholz, P. Wust, H. Fahling, R. Felix, *J. Magn. Magn. Mater.*, 1999, **201**, 413.
62. M. Bruchez, Jr. M. Moronne, P. Gin, S. Weiss, A. P. Alivisatos, *Science*, 1998, **281**, 2013.
63. Carpenter, J. *J. Magn. Magn. Mater.* 2001, **225**, 17.
64. N. Zhao, M. Gao, *Adv. Mater.* 2009, **21**, 184–187.
65. R. K. Shah, J.-W. Kim, D. A. Weitz, *Adv. Mater.*, 2009, **21**, 1949–1953.
66. A. K. F. Dyab, M. Ozmen, M. Ersoz, V. N. Paunov, *J. Mater. Chem.*, 2009, **19**, 3475–3481.
67. L. B. Zhao, L. Pan, K. Zhang, Guo, S. S. Liu, W. Y. Wang, Y. Chen, X. Z. Zhao, H. L. W. Chan, *Lab Chip*, 2009, **9**, 2981–2986.
68. S. K. Smoukov, S. Gangwal, M. Marquez, O. D. Velev, *Soft Matter*, 2009, **5**, 1285–1292.
69. T. Neuberger, B. Schopf, H. Hofmann, M. Hofmann, B. von Rechenberg, *J. Magn. Magn. Mater.*, 2005, **293**, 483–496.
70. S. Seiffert, M. B. Romanowsky, and D. A. Weitz, *Langmuir*, 2010, **26**, 14842–14847.
71. C. H. Chen, R. K. Shah, A. R. Abate, and D. A. Weitz, *Langmuir*, 2009, **25**, 4320–4323.
72. A. R. Abate, A. T. Krummel, D. Lee, M. Marquez, C. Holtze, D. A. Weitz, *Lab Chip*, 2008, **8**, 2157–2160.
73. H. C. Shum, A. R. Abate, D. Lee, A. R. Studart, B. Wang, C. H. Chen, J. Thiele, R. K. Shah, A. Krummel, D. A. Weitz, *Macromol. Rapid Commun.*, 2010, **31**, 108–118.
74. C. H. Chen, A. R. Abate, D. Lee, E. M. Terentjev, and D. A. Weitz, *Adv. Mater.*, 2009, **21**, 3201–3204.
75. S. Lone, S. H. Kim, S. W. Nam, S. Park, and I. W. Cheong, *Langmuir*, 2010, **26**, 17975–17980.

**Abstract:** This review presents a short [description](#) of the polymeric Janus particles fabricated by droplet microfluidics.

